CHINESE OPTICS LETTERS

Vol. 21, No. 11 | November 2023

Nd:YAG linearly polarized laser based on polarization eigenmodes

Jing Wang (王 晶)[1,2], Kaifei Tang (汤凯飞)[1], Bingxuan Li (李丙轩)[1,2,3*], and Ge Zhang (张 戈)[1,2,3**]

[1] Fujian Institute of Research on the Structure of Matter, Chinese Academy of Sciences, Fuzhou 350002, China

[2] University of Chinese Academy of Sciences, Beijing 100049, China

[3] Fujian Science and Technology Innovation Laboratory for Optoelectronic Information of China, Fuzhou 350108, China

*Corresponding author: libingxuan@fjirsm.ac.cn

**Corresponding author: zhg@fjirsm.ac.cn

Received May 25, 2023 | Accepted July 6, 2023 | Posted Online November 6, 2023

In this paper, the frequency difference of the eigen polarization modes of the Nd:YAG crystal laser at different polarization ratios is experimentally studied, and to the best of our knowledge, the correlation between the frequency difference of the eigenmodes and the output polarization degree is reported for the first time. Combined with the analysis of the polarization beam profile, it is proved that the polarized laser produced by the isotropic crystal is due to the frequency locking of the eigen polarization modes. The weak birefringence in the crystal causes the round-trip phase difference of the orthogonal polarization modes, which leads to the frequency difference between the polarization modes. By the adjustment of the cavity mirror, the anisotropic loss will interact with the round-trip phase difference. The eigen polarization modes can reach frequency degeneration, and then be coherently combined to produce linearly polarized laser output. This work provides a useful reference for understanding the physical mechanism of polarized lasers realized by isotropic crystals.

Keywords: linear polarization; frequency difference; weak birefringence.

DOI: 10.3788/COL202321.111401

1. Introduction

The YAG crystal belongs to the cubic crystal system and is generally considered to be optically isotropic[1]. Therefore, when the rare-earth-doped YAG laser does not use an anisotropic optical element in the cavity, the output laser has no specific polarization orientation. Because of the weak birefringence, which is generally caused by weak stress, these lasers are orthogonal and dual-polarized[2]. However, since 1987, Nd:YAG[3,4], Tm:YAG[5], Er:YAG[6], and Yb:YAG[7] have achieved polarization control laser output. Kravtsov *et al.* studied the influence of the polarization of the pump light in the isotropic cavity on the degree of polarization of the laser output[8]. By rotating the angle of the laser crystal, Dong *et al.* realized the self-selective linearly polarized laser output consistent with the crystal axis direction in the Yb:YAG microchip laser and also in the Cr:Nd:YAG and Yb:YAG/Cr^{4+} *Q*-switched laser[9–11]. Dong *et al.* used the anisotropy of the crystal axis direction to realize the linearly polarized laser output of the Yb:YAG microchip[12]. Otsuka and Chu achieved a polarization output consistent with the pump polarization in Nd:YAG ceramics[13,14]. In 2014, by fine-tuning the laser cavity, Li realized a linearly polarized laser with a high degree of polarization independent of the crystal orientation and pump polarization in the YAG/Tm:YAG/YAG laser crystal[5].

The explanation of the linearly polarized radiation behavior directly produced by the isotropic solid-state laser generally uses the analysis of the local symmetry of the dopant ion distribution in the matrix crystal[12,15-18]. This analysis only yields a slight difference in gain or loss. It is not sufficient for explaining the selective output of the laser polarization mode. In our previous work, the output polarized laser was proved to be a coherent superposition of two eigen polarization modes by the analysis of the polarized spot profile[19,20]. Although the experimental results are in good agreement with the explanation, the specific frequency difference changes are not measured and analyzed, which is important evidence. In order to fully verify the correctness of the analysis, this paper measured the frequency difference between the polarization modes under different polarization ratios. The route of the frequency locking between two polarization modes was clearly observed, which proved that the polarized laser output of the isotropic Nd:YAG laser is the frequency locking and coherent superposition of two polarization modes.

2. Theoretical Analysis

The coherent combination of two polarized lights means that their frequencies are the same[21]. Brunel has proved that in a

near isotropy cavity, by adjusting the relative amount and direction of weak phase and loss anisotropies, the frequency difference between two eigen polarization modes will be reduced[22]. When the angle between the axes of these two anisotropies is 45° and the loss anisotropy is larger than the phase anisotropy, the frequency difference will fall into the locked region, which is called frequency degeneration[23–26]. It provides the possibility to coherently combine the two eigenmodes into the linear polarization.

The Jones matrix of a round trip[20,27] corresponding to the above mentioned cavity is given by

$$M(\Delta\varphi,\Delta T)=\begin{pmatrix} e^{-i\Delta\varphi} & 0 \\ 0 & 1 \end{pmatrix}\begin{pmatrix} 1 & -\Delta T \\ \Delta T & 1 \end{pmatrix}\begin{pmatrix} 1 & 0 \\ 0 & e^{i\Delta\varphi} \end{pmatrix}, \quad (1)$$

where the $\Delta\varphi$ is the round-trip phase difference caused by weak birefringence, and ΔT is the loss anisotropy. The angle between the axes of the phase and the loss anisotropies is 45°.

The eigenvalues of the matrix are calculated to be

$$\lambda_{\pm}=\cos\ \Delta\varphi \pm \sqrt{\delta}, \quad (2)$$

where $\delta=\Delta T^2-(\sin\ \Delta\varphi)^2$.

The corresponding eigenstates of polarization are

$$E_{\pm}=\frac{1}{\sqrt{1+\Delta T^2}}\begin{bmatrix} 1 \\ (\pm\sqrt{\delta}-i\ \sin\ \Delta\varphi)/\Delta T \end{bmatrix}. \quad (3)$$

When $\delta<0$, the eigenvalues are conjugate complex numbers. Then, the frequency difference of the two eigenstates must be

$$\Delta\nu=2\pi\ \arccos\left(\frac{\cos\ \Delta\varphi}{\sqrt{1-\Delta T^2}}\right)\frac{c}{L}, \quad (4)$$

where c is velocity of light, and L is the optical length of the cavity.

When $\delta\geq 0$, the eigenvalues are real numbers. In this case, the frequency of the eigenstates is the same.

The relationship between $\Delta\nu$ and ΔT in the case of fixed $\Delta\varphi$ is calculated and shown in Fig. 1.

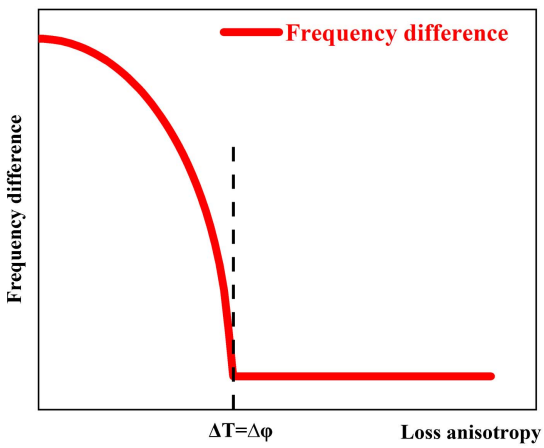

Fig. 1. The relationship between the theoretical simulation frequency difference and the loss anisotropy.

As shown in Fig. 1, when the phase anisotropy $\Delta\varphi$ is fixed, the frequency difference begins to decrease as the loss anisotropy ΔT increases. When the loss anisotropy ΔT is greater than or equal to the phase anisotropy $\Delta\varphi$, the frequency difference is zero. The continued increase of loss anisotropy ΔT will not change the state of frequency degeneracy. The frequency difference with the phase anisotropy and loss anisotropy is important evidence for verifying the frequency locking of the polarized eigenmodes.

3. Experiment Design

The experimental device is shown in Fig. 2. A fiber-coupled semiconductor laser diode (LD) with a center wavelength of 808 nm produced by LIMO is used as a pumping source. The numerical aperture of the fiber is 0.22, and the fiber core diameter is 200 μm. The pump light is collimated and incident on the end face of the gain medium by a pair of plano-convex lenses, and the coupling ratio of the shaping system is 1:2. The gain medium used in the experiment is a Nd:YAG crystal with the Nd^{3+} doping concentration of 1% and the size of 3 mm × 3 mm × 10 mm. One coated surface of the Nd:YAG crystal S1 has high transmittance to the pump light at 808 nm as well as high reflectivity to 1064 nm ($R>99.93\%$), and the other coated surface S2 has a high transmittance to 808 nm and 1064 nm. In order to achieve good crystal temperature control, the crystal is wrapped with indium foil and placed on a copper block and cooled by a thermoelectric cooler (TEC) module. The temperature is controlled at about 286.5 K. The output coupling mirror M1 is coated with a transmittance of 10% at 1064 nm wavelength. It is placed on a movable platform to adjust the cavity length. The length of the laser cavity is controlled between 20 and 150 mm. The pump light is filtered from the output laser through the M2 filter, which is highly reflective to 808 nm and highly transparent to the 1064 nm wavelength. The Glan prism is used as a polarization analyzer (transmission range 350–2300 nm). The laser power with different polarization characteristics is measured by the power meter. The beam profile is measured by a charge coupled device (CCD). The power spectrum of the output power is measured by a spectrum analyzer, which consists of a silicon-based photodetector (Thorlabs DET025A/M) and spectrum analyzers (Keysight N9000A).

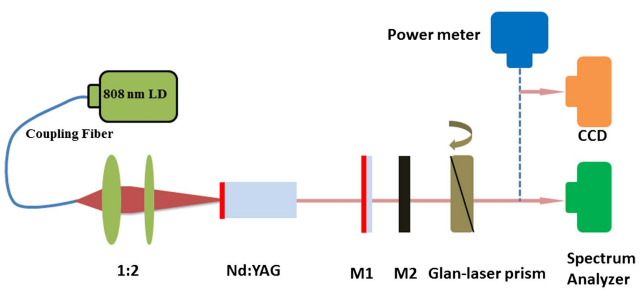

Fig. 2. Schematic diagram for the operation and measurement of the linear polarization regime of the continuous-wave Nd:YAG laser.

4. Results and Discussion

The free-running output power without the Glan prism and the power corresponding to the angle of the Glan prism are shown in Fig. 3. The maximum output power is 0.323 W at the pump power of 1.37 W. By rotating the angle of the Glan prism, the polarization of the output power is found to be near unpolarized.

The frequency difference variations with the angle of the analyzer in the case of the free-running state are shown in Fig. 4. As shown in Fig. 4(a), in the power spectrum, there exist some signal peaks whose signal intensity varies under the analyzer of 10°, 20°, and 30° in the case of the free-running state. As shown in Fig. 4(b), the intensity varies from zero to maximum with the detecting angle range of 45°. This can be explained by the beating of the two eigen polarization modes. There are two eigen polarization modes in the cavity. In the case of the free-running state, the frequency difference between them will not change with the detecting angle, but the beating frequency intensity will change. When the analyzer direction coincides with a certain eigen polarization mode, since the component of the other eigen polarization mode is almost nothing, the beating intensity of these two modes should be near zero. When the angle between the analyzer direction and the eigen polarization mode is 45°, the components of the two eigen polarization modes in the analyzer direction are equal, and then the intensity of the beating signal should be the largest. Based on the above analysis, the direction of the eigen polarization mode can be measured in the case of the free-running state. The change of the frequency beating with the analyzer angle is tested at different positions of the Nd:YAG. At different positions, the direction of the eigen polarization mode is different. We selected a position whose direction of the eigen polarization mode is 45° away from the horizontal direction to further carry out the experiment.

By finely adjusting the cavity mirrors horizontally, a near linearly polarized laser can be obtained, which is shown in Fig. 5. The maximum output power is 0.312 W at a pump power of 1.37 W. By rotating the angle of the Glan prism, the polarization of the output power is found to be near linear. Through

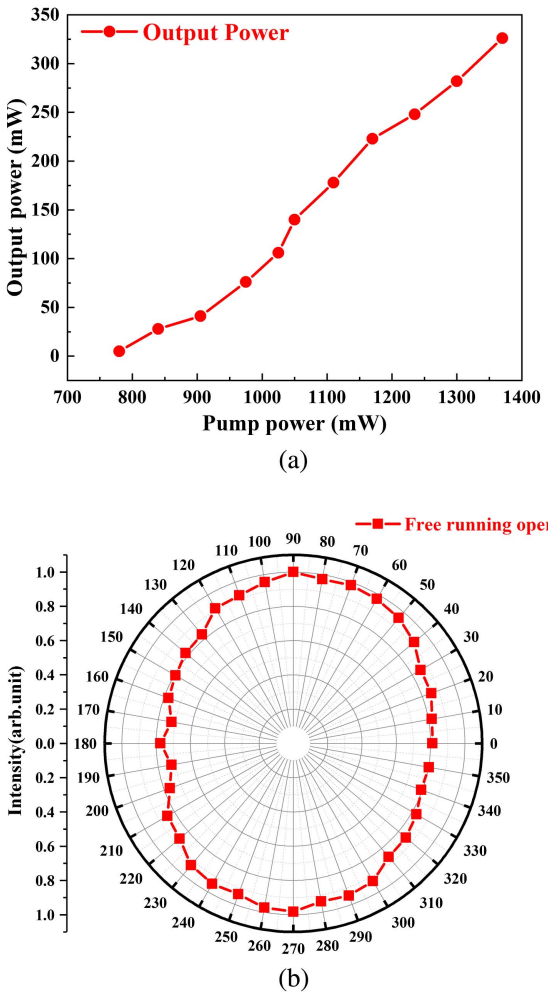

Fig. 3. Output power of the free-running state (a) without the Glan prism and (b) after the corresponding angle of the Glan prism.

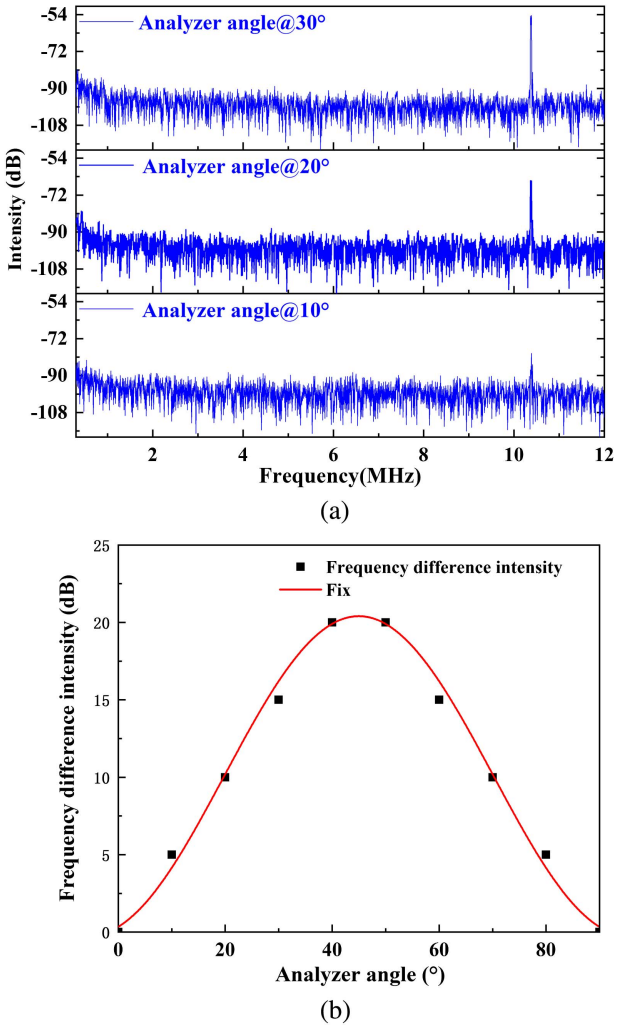

Fig. 4. The frequency difference varies with the angle of the analyzer in the case of the free-running state. (a) The power spectrum under the analyzer of 10°, 20°, and 30°. (b) The relationship between the frequency difference intensity and the angle of the analyzer.

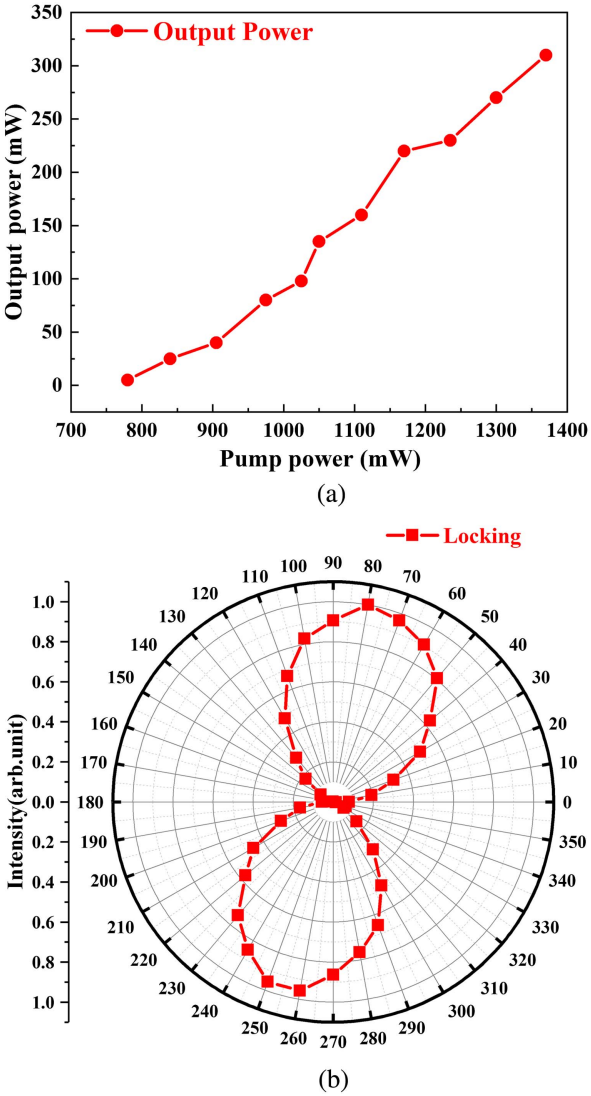

Fig. 5. Polarization output characteristics of the near linearly polarized laser (a) without the Glan prism and (b) after the corresponding angle of the Glan prism.

the maximum power P_1 and the minimum power P_0, the polarization extinction ratio (PER) of the polarized light can be defined as PER = $10 \times \lg(P_1/P_0)$ (dB) and is usually expressed in decibels. As high as 31 dB of the PER can be achieved in the experiment.

The beating frequency of the two eigen modes was measured during the adjusting. The variation was clearly observed. As shown in Fig. 6, the frequency difference decreases and suddenly disappears during the transition from the free-running state to the frequency locking state. As shown in Fig. 7, the PERs corresponding to the frequency differences are recorded in detail during the experiment. The experimental results show that as the PER increases, the frequency difference decreases and suddenly disappears, which indicates frequency locking.

The relationship between the PER and the beating frequency is shown in Fig. 8. The frequency difference in the free-running

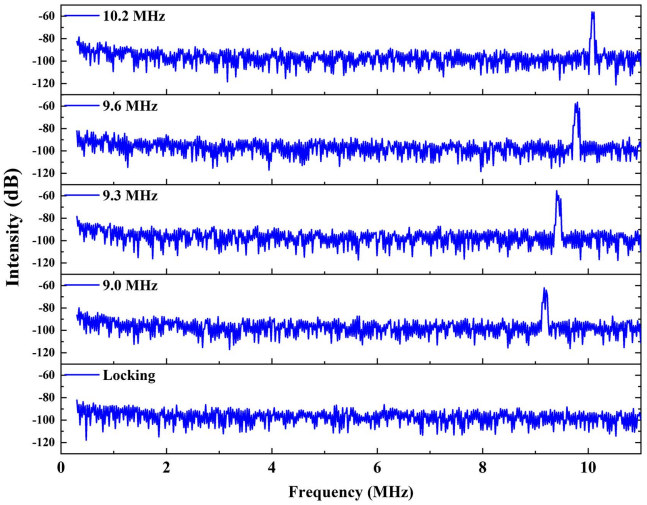

Fig. 6. The change of the frequency difference during the transition from the free-running state to the frequency locking state.

state is 10.2 MHz. By adjusting the output coupler (OC), the frequency difference begins to decrease, from 10.2 MHz to 9.6 MHz, and the PER is 4.1 dB. Continuing to adjust the OC, the beating frequency is reduced to 9.3 MHz, and the PER becomes 8.9 dB. When the PER reaches 20.1 dB, the beating frequency is reduced to 9.0 MHz. After that, finely tuning the OC, the beating frequency suddenly disappears. The extinction ratio at this time reaches 31 dB. It can be seen that with the fine adjustment of the OC, the frequency difference between the two eigen polarization modes begins to decrease in a small range, and the PER of the output laser rises sharply. When the frequency difference is reduced to about 9 MHz, the tiny OC adjustment can realize the complete disappearance of the frequency difference, and the PER reaches a maximum of 31 dB.

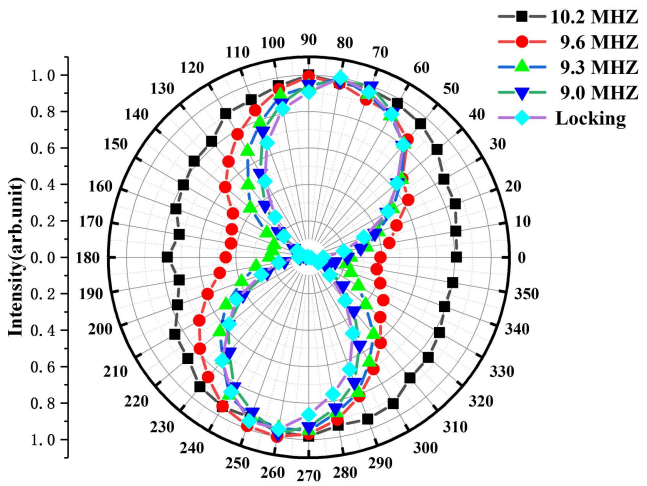

Fig. 7. The change of the polarization curve during the transition from the free-running state to the frequency locking state.

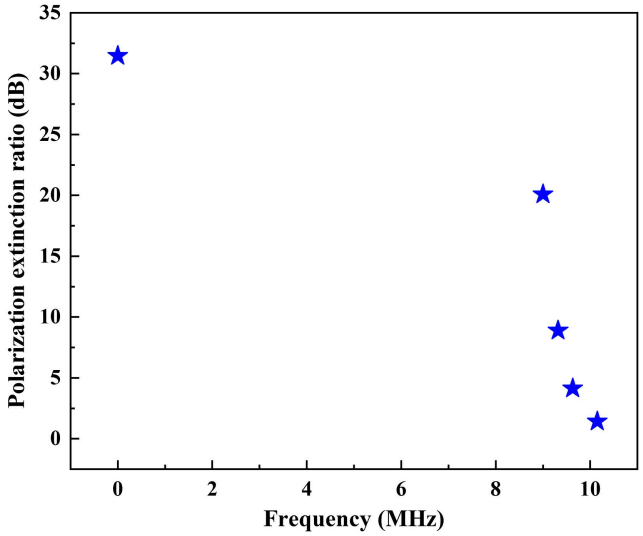

Fig. 8. The relationship between the degree of polarization and the frequency difference during the transition from the free-running state to the frequency locking state.

We further studied the influences of different OC transmittances on the polarization frequency using the OC transmittances of 5%, 10%, 15%, 20%, and 30%, respectively. The optical axis is consistent with the last time after replacing the output mirror. As shown in Fig. 9(a), with the change of the OC transmittance, experiments show that the realization of the linearly polarized laser does not depend on the coupling rate of the OC. In the next step, the influence of different cavity lengths on the polarization state of the output laser was studied. The adjustment range of the cavity length L is 20–150 mm, and the step size is 10 mm. The optical axis is consistent with the last time after changing the cavity length. As shown in Fig. 9(b), with the adjustment of the cavity length, the experiment shows that the realization of the linearly polarized laser does not depend on the cavity length.

The beam profile of spontaneous polarization output in the free-running state and the maximum PER is analyzed. After the output laser passes through the analyzer, the beam profile under different rotation angles of the analyzer is recorded by the CCD. The prism is gradually rotated to different directions relative to the polarization direction, and the variations of the profile are observed and shown in Fig. 10.

In Case 1, it is a laser with unpolarized output, the obtained spot has nothing to do with the direction of the Glan prism, and it is a circle. Case 2 is the laser output of the maximum PER. When the Glan prism is exactly in the extinction direction of the polarized laser, four spots can be observed in the figure. When the prism is slightly deviated from the extinction position, there is only one oblique irregular ellipse at the left- and right-skewed position. Moreover, the major axes of a pair of elliptical spots approximately intersect.

As shown in Fig. 11, using the same calculation of reference[20], by changing the ellipticity parameters and position parameters, various dislocations of the two eigenmodes are

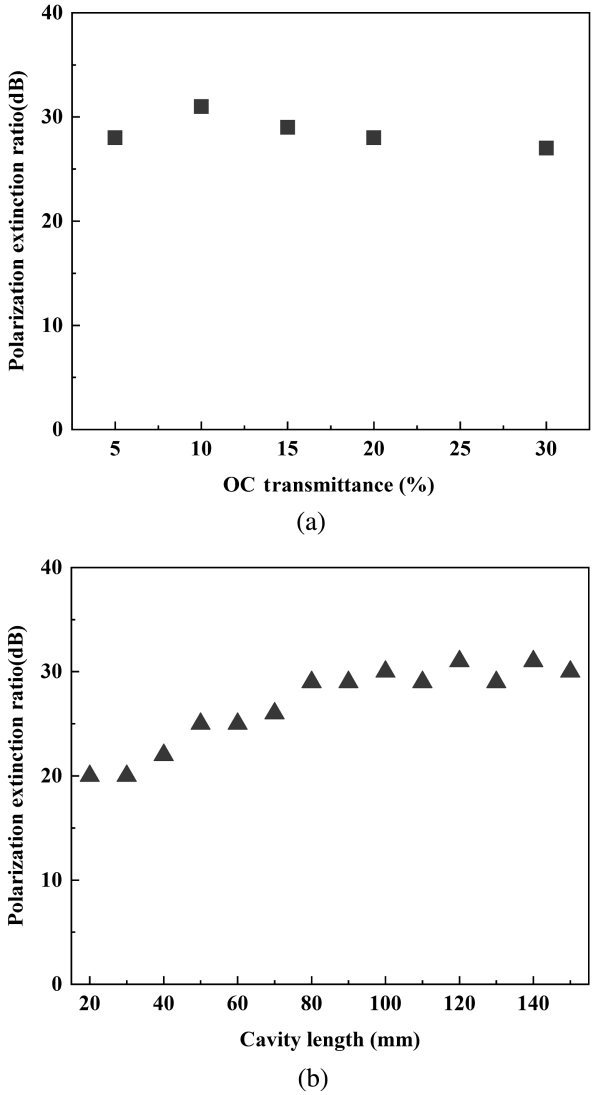

Fig. 9. The relationship between the linearly polarized laser realization and (a) the output transmittance and (b) the cavity length.

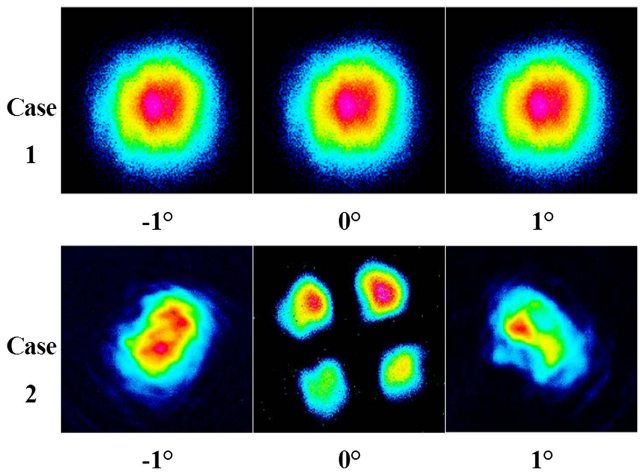

Fig. 10. Experimental test of two beam profile changes.

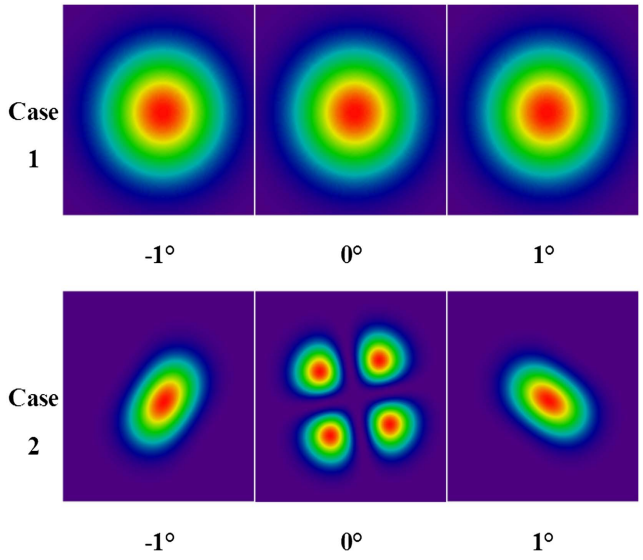

Fig. 11. Theoretical simulation of two beam profile changes.

simulated. The experimental results are well consistent with the theoretical simulation.

5. Conclusion

The frequency difference of the eigen polarization modes was determined by the power spectrum analysis during the generation of a linearly polarized output laser with an isotropic Nd:YAG crystal. The frequency difference of the eigenmodes, which is caused by the weak anisotropy inside the crystal, was clearly observed to be reduced with the tiny adjustment of the cavity. The locking route can be clearly shown on the power spectrum. The frequency locking of the eigen polarization modes was experimentally proved to be the physical mechanism of the polarized output with isotropic laser media.

Acknowledgement

This work was supported by the Youth Innovation Promotion Association CAS (No. 2022303), the CAS Key Technology Talent Program (No. 2022000061), the National Natural Science Foundation of China (Nos. U21A20508, 61975208, and 62105334), the Scientific Instrument Developing Project of the Chinese Academy of Sciences (No. YZLY202001), the Fujian Science and Technology Innovation Laboratory for Optoelectronic Information of China (Nos. 2021ZR203, 2020ZZ108, and 2021ZZ118), and the Project of Science and Technology of Fujian Province (No. 2021H0047).

References

1. W. A. Clarkson and D. C. Hanna, "Efficient Nd:YAG laser end pumped by a 20-W diode-laser bar," Opt. Lett. **21**, 869 (1996).
2. A. Le Floch, G. Ropars, J. M. Lenormand, and R. Le Naour, "Dynamics of laser eigenstates," Phys. Rev. Lett. **52**, 918 (1984).
3. A. Owyoung and P. Esherick, "Stress-induced tuning of a diode-laser-excited monolithic Nd:YAG laser," Opt. Lett. **12**, 999 (1987).
4. S. Chen, J. Li, S. Zhou, H. Zhao, and K.-i. Ueda, "Generation of vector polarization in a Nd:YAG laser," Opt. Express **27**, 15136 (2019).
5. Y. Li, W. Chen, H. Lin, D. Ke, G. Zhang, and Y.-F. Chen, "Manipulation of linearly polarized states in a diode-pumped YAG/Tm:YAG/YAG bulk laser," Opt. Lett. **39**, 1945 (2014).
6. R. Song, X. Liu, S. Fu, and C. Gao, "Simultaneous tailoring of longitudinal and transverse mode inside an Er:YAG laser," Chin. Opt. Lett. **19**, 111404 (2021).
7. M. Rumpel, A. Voss, M. Moeller, F. Habel, C. Moormann, M. Schacht, T. Graf, and M. A. Ahmed, "Linearly polarized, narrow-linewidth, and tunable Yb:YAG thin-disk laser," Opt. Lett. **37**, 4188 (2012).
8. N. V. Kravtsov, E. G. Lariontsev, and N. I. Naumkin, "Dependence of polarisation of radiation of a linear Nd:YAG laser on the pump radiation polarisation," Quantum Electron. **34**, 839 (2004).
9. J. Dong, P. Deng, Y. Lu, Y. Zhang, Y. Liu, J. Xu, and W. Chen, "Laser-diode-pumped Cr^{4+},Nd^{3+}:YAG with self-*Q*-switched laser output of 1.4 W," Opt. Lett. **25**, 1101 (2000).
10. J. Dong, J. Ma, and Y. Y. Ren, "Polarization manipulated solid-state lasers with crystalline-orientations," Laser Phys. **21**, 2053 (2011).
11. J. Dong, G. Xu, J. Ma, M. Cao, Y. Cheng, K.-i. Ueda, H. Yagi, and A. A. Kaminskii, "Investigation of continuous-wave and *Q*-switched microchip laser characteristics of Yb:YAG ceramics and crystals," Opt. Mater. **34**, 959 (2012).
12. J. Dong, A. Shirakawa, and K.-i. Ueda, "A crystalline-orientation self-selected linearly polarized Yb:$Y_3Al_5O_{12}$ microchip laser," Appl. Phys. Lett. **93**, 101105 (2008).
13. K. Otsuka and T. Ohtomo, "Polarization properties of laser-diode-pumped micro-grained Nd:YAG ceramic lasers," Laser Phys. Lett. **5**, 659 (2008).
14. K. Otsuka, K. Nemoto, K. Kamikariya, Y. Miyasaka, and S.-C. Chu, "Linearly polarized single-frequency oscillations of laser-diode-pumped microchip ceramic Nd:YAG lasers with forced Ince–Gaussian mode operations," Jpn. J. Appl. Phys. **46**, 5865 (2007).
15. A. V. Volyar, A. P. Kiselev, and Y. A. Egorov, "Eigen-polarization beams in uniaxial crystals," Proc. SPIE **5582**, 98 (2004).
16. A. Kul'Minskii, R. Vilaseca, and R. Corbalán, "Full polarization chaos in a pump-polarization modulated isotropic cavity laser," Opt. Lett. **20**, 2390 (1995).
17. N. B. Abraham, E. Arimondo, and M. San Miguel, "Polarization state selection and stability in a laser with a polarization-isotropic resonator; an example of no lasing despite inversion above threshold," Opt. Commun. **117**, 344 (1995).
18. M. Lukac, S. Trost, and M. Kazic, "Flip-flop polarization effect in cube-corner-flat cavity Nd:YAG laser," IEEE J. Quantum Electron. **28**, 2560 (1992).
19. K. Tang, W. Liao, D. Lin, B. Li, W. Chen, and G. Zhang, "Self-polarization emission based on coherent combination of intracavity eigenmodes in Nd:YAG/Cr^{4+}:YAG lasers," Chin. Opt. Lett. **19**, 021401 (2021).
20. K. Tang, W. Liao, K. Li, B. Li, W. Chen, and Z. Ge, "Coherent combination of two intracavity eigenmodes producing linearly polarized emission in an isotropic laser," Opt. Express **28**, 34337 (2020).
21. Purnawirman and P. B. Phua, "High power coherent polarization locked laser diode," Opt. Express **19**, 5364 (2011).
22. M. Vallet, M. Brunel, F. Bretenaker, M. Alouini, A. Le Floch, and G. P. Agrawal, "Polarization self-modulated lasers with circular eigenstates," Appl. Phys. Lett. **74**, 3266 (1999).
23. M. Brunel, O. Emile, M. Alouini, A. Le Floch, and F. Bretenaker, "Self-mode-locked pulsed monomode laser," Opt. Lett. **24**, 229 (1999).
24. M. Vallet, M. Brunel, G. Ropars, A. Le Floch, and F. Bretenaker, "Theoretical and experimental study of eigenstate locking in polarization self-modulated lasers," Phys. Rev. A **56**, 5121 (1997).
25. M. Brunel, M. Vallet, G. Ropars, A. Le Floch, F. Bretenaker, G. Jouliéand, and J.-C. Keromnes, "Modal analysis of polarization self-modulated lasers," Phys. Rev. A **55**, 1391 (1997).
26. M. Brunel, M. Vallet, A. Le Floch, and F. Bretenaker, "Differential measurement of the coupling constant between laser eigenstates," Appl. Phys. Lett. **70**, 2070 (1997).
27. Y. Zhao, B. Wang, and Q. Tang, "Jones matrix for round-trip wave-propagation in nonreciprocal media," Appl. Opt. **31**, 4471 (1992).